Relationship between installation torque and uplift capacity of deep helical piles in sand

Cristina de Hollanda Cavalcanti Tsuha and Nelson Aoki

Abstract: The empirical torque correlation factor (K_T), which relates the uplift capacity to the installation torque of helical piles, is routinely used as an on-site instrument for quality control with this type of foundation. This paper presents a theoretical relationship between uplift capacity and installation torque of deep helical piles in sand. An experimental program, including centrifuge and direct shear interface tests, was carried out to validate this expression. The experimental results were compared with the values predicted by the suggested approach and showed good agreement. As the developed model depends on the residual interface friction angle (δ_r) between the helix surface and the surrounding sand, results of δ_r, extracted from different sand samples, are presented for use in this suggested relationship on site. Also, the values of K_T found in this work were compared with those of field and laboratory tests on helical piles in sand reported in the literature. From this analysis, it was found that the measured values of K_T decrease with an increase in pile dimensions and, in most of cases, with an increase in sand friction angle. These results were explained by the presented model.

Key words: helical screw piles, uplift capacity, torque correlation factor, sand, centrifuge modeling, residual interface friction angle.

Résumé : Le facteur empirique de corrélation du torque K_T, qui représente la capacité de soulèvement du torque d'installation de pieux hélicoïdaux, est généralement utilisé comme instrument de contrôle de la qualité sur le terrain pour ce type de fondations. Dans cet article, une relation théorique entre la capacité de soulèvement et le torque d'installation de pieux hélicoïdaux placés profondément dans du sable est présentée. Un programme expérimental, qui comprend des essais centrifuge et de cisaillement direct à l'interface, a été effectué dans le but de valider cette relation théorique. Les résultats expérimentaux ont été comparés aux résultats prédits par l'approche suggérée, et les résultats montrent une bonne concordance. Puisque le modèle développé dépend de l'angle de friction résiduel à l'interface δ_r entre la surface de l'hélice du pieu et le sable, les résultats de δ_r obtenus à partir de différents échantillons de sable sont présentés afin d'être utilisés lors de l'application sur le terrain de la relation théorique proposée. De plus, les valeurs de K_T obtenues dans ces travaux ont été comparées à celles reportées dans la littérature; celles-ci ayant été obtenues lors d'essais sur le terrain et en laboratoire sur des pieux hélicoïdaux dans le sable. Cette analyse a permis de démontrer que les valeurs mesurées de K_T diminuent lorsque la dimension des pieux augmente, ainsi qu'avec une augmentation de l'angle de friction du sable, dans la plupart des cas. Ces derniers résultats ont aussi été démontrés avec le modèle présenté.

Mots-clés : pieux hélicoïdaux vissés, capacité de soulèvement, facteur de corrélation du torque, sable, modélisation centrifuge, angle de friction résiduel à l'interface.

[Traduit par la Rédaction]

Introduction

Helical screw piles are installed in soil by applying a torque to the upper end of the shaft by mechanical means.

Commonly, the uplift capacity of helical piles has been controlled by the torsional resistance to the pile penetration measured during installation. This installation effort is used as a tool to evaluate foundation quality. This procedure is based on the empirical torque correlation factor (K_T), which relates the uplift capacity to the torque required to install helical piles to the desired depth, although a number of theoretical correlations have been reported in the literature (Narasimha Rao et al. 1989; Ghaly et al. 1991; Ghaly and Hanna 1991; Ghaly 1995; Perko 2000).

Zhang (1999) stated that this empirical relationship is supported by statistical analysis based on a large database and is widely used in the industry to predict the uplift capacity of screw anchors because it is simple to use and provides a procedure to verify if the predicted design loads have been reached at the site location. Hargrave and Thorsten (1992) mentioned that K_T is also applied to estimate pile compression capacity. Livneh and El Naggar (2008) cited that this correlation has long been used in the field, with the rationale that the installation torque is a measure of energy required to overcome the shear strength of the soil and is hence directly relate to pile capacity.

Pack (2003) reported that, although design information of this pile type is available in the literature, detailed information on quality control, inspection, and performance monitoring is lacking. Therefore, this paper presents in detail the simplified theoretical relationship developed by Tsuha

Received 9 October 2008. Accepted 14 October 2009. Published on the NRC Research Press Web site at cgj.nrc.ca on 26 May 2010.

C. de H.C. Tsuha[1] and N. Aoki. Department of Geotechnics, São Carlos School of Engineering, University of São Paulo, Av. Trabalhador Saocarlense 400, CEP 13566-590, São Carlos SP, Brazil.

[1]Corresponding author (e-mail: crishc@terra.com.br).

Fig. 1. Scheme of the hypotheses assumed by Tsuha (2007): (*a*) driving and resisting moments acting during pile installation; (*b*) forces resisting to the upward movement.

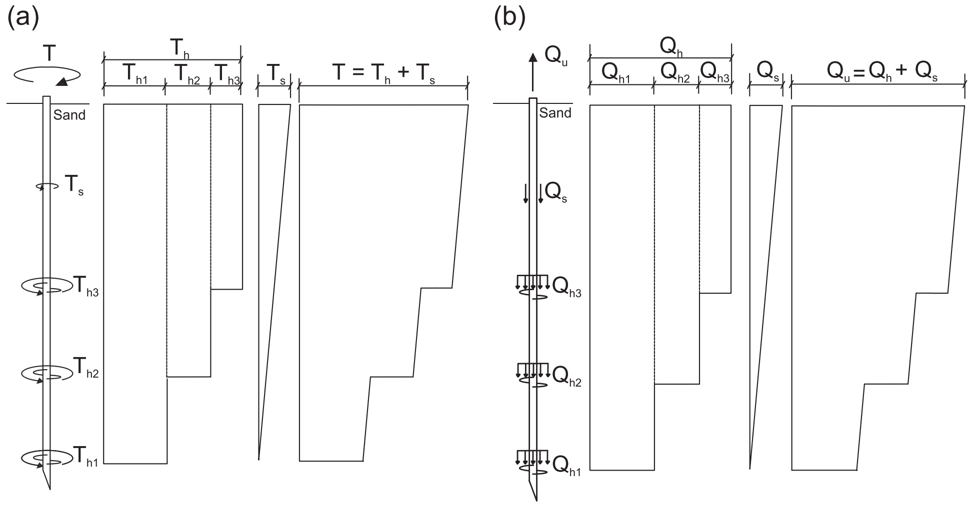

Fig. 2. Resisting forces and moments acting on the helix surfaces at a given installation depth.

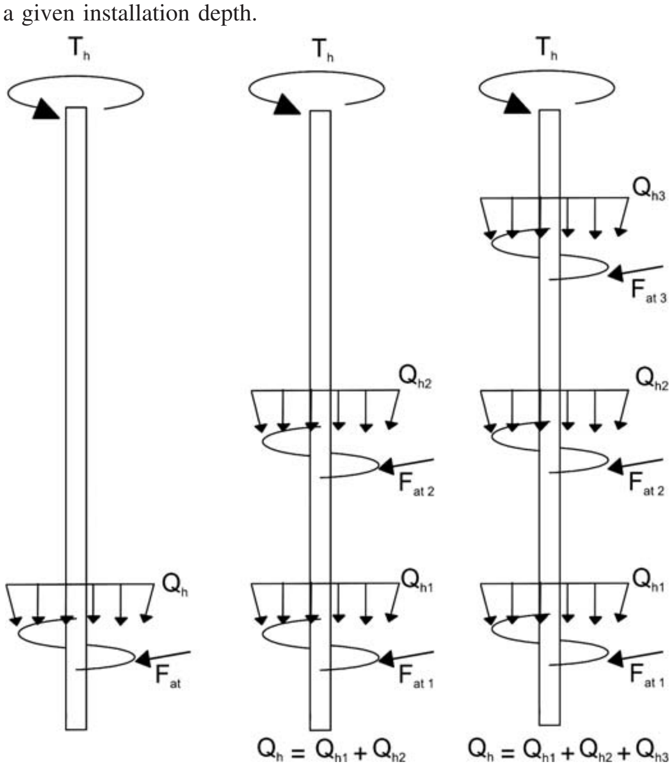

(2007) and recommended for deep helical piles in sand which correlates the uplift capacity with the installation torque. This equation expresses the physical mean of the empirical relationship symbolized by K_T. A series of centrifuge model tests were performed on 12 types of model piles installed in two sand samples with different relative densities to validate the component of this proposed expression related to the contribution of helical plates to the uplift capacity. The pile installation, with measures of the resisting torque, and pull-out tests were conducted in-flight.

The residual friction angle between the helix surface and the surrounding sand is a fundamental parameter of the theoretical relationship described in this work. Consequently, a testing programme of direct shear interface tests was conducted to find the residual interface friction angle between the helix material and the surrounding sand employed in centrifuge tests. In addition, direct shear interface tests between a helical plate material used in full-scale piles and different sand samples were carried out to provide results to be employed in the application of the present model to control on site the uplift capacity of helical piles with similar sand–steel interface characteristics.

The measured values of K_T found in the present investigation were compared with the field and laboratory values reported in the literature.

Theoretical relationship

The theoretical model proposed by Tsuha (2007) assumes that the resisting moments acting on a three-helix helical pile during installation in sand are those shown in Fig. 1*a*.

The torque required to install the helical pile (T), presented in Fig. 1*a*, can be given by the following expression:

$$[1] \qquad T = T_h + T_s$$

where T_s is the resisting moment acting on the pile shaft; and T_h is the resisting moment acting on the helices, which is expressed as

$$[2] \qquad T_h = \sum_{i=1}^{N} T_{hi}$$

where T_{hi} is the resisting moment acting on helix i, i is the index from 1 to N, and N is the number of helices.

The forces resisting the upward movement of a three-helix helical pile in sand assumed in this approach are shown in Fig. 1*b*. Considering that this method is suggested for deep helical piles, the uplift capacity is equal to the sum of the capacities of individual helices and the shaft resistance. The variation of shaft resistance along the pile was not considered in the simplified scheme illustrated in Fig. 1.

The present model assumes that failure occurs above each individual helix as considered in the A.B. Chance Co.

Fig. 3. Adjustment of the power screw mechanism to helical piles (Tsuha 2007).

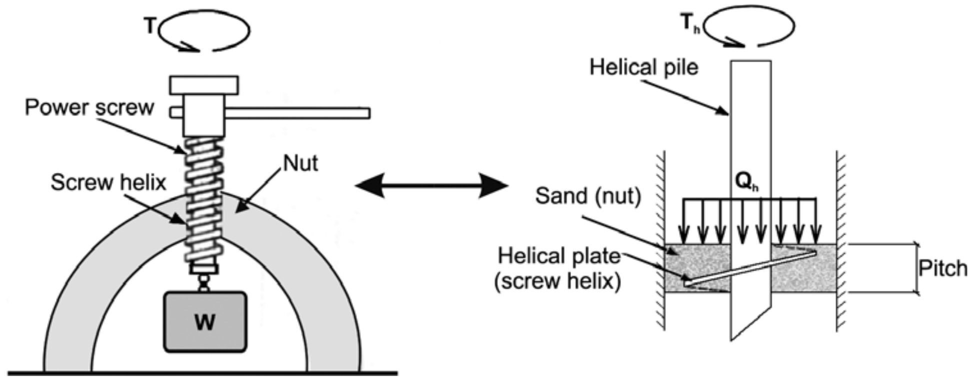

Fig. 4. Forces acting on the upper surface of a screw element: (*a*) body moving up an incline (Faires 1943); (*b*) helix surface during helical pile installation in sand.

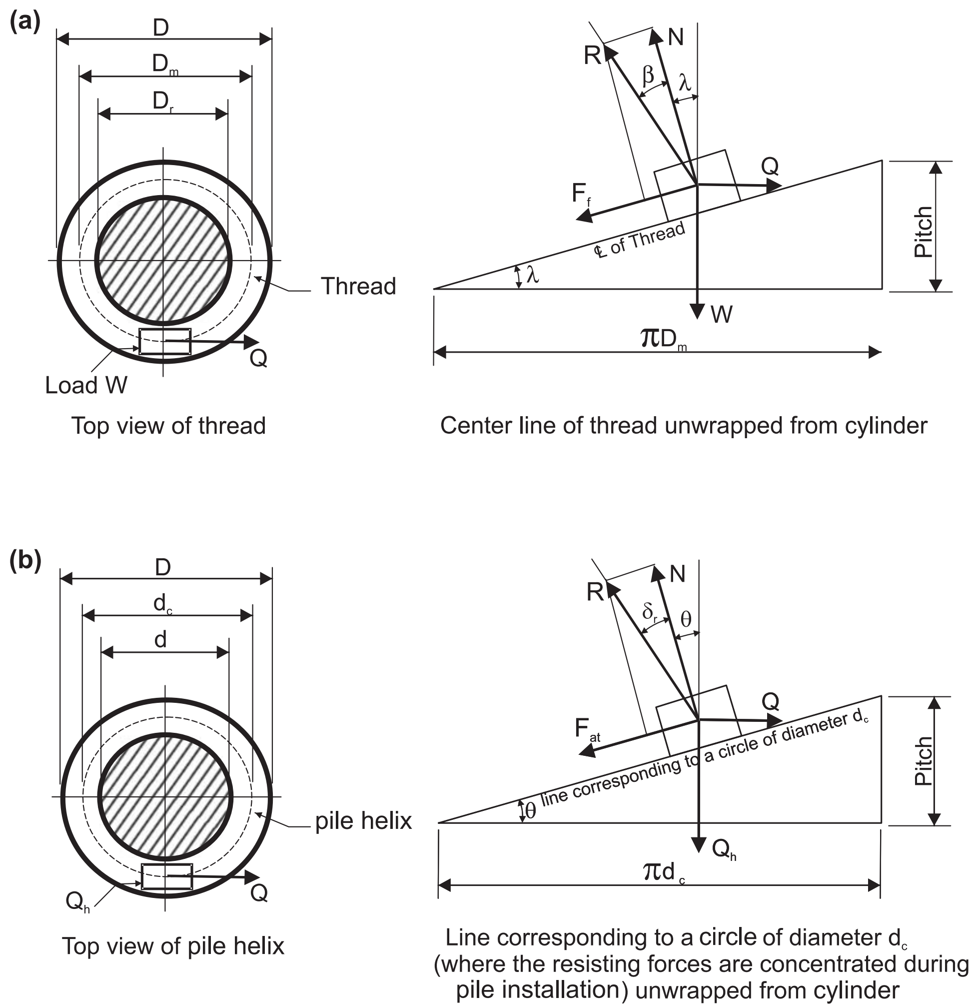

method reported by Clemence et al. (1994). Based on the A.B. Chance Co. method, the proposed theoretical relationship is recommended for helical piles in which the space between any two helices is greater than three times the helix diameter. Adams and Klym (1972) stated that each helical plate can be assumed to behave independently of the other when the vertical spacing of the plates is at least twice the diameter of the plates.

The uplift capacity (Q_u), which is shown in Fig. 1*b*, can be given by the following equation:

$$[3] \qquad Q_u = Q_s + Q_h$$

Table 1. Sand properties.

Maximum dry density (kN/m^3)	16.68
Minimum dry density (kN/m^3)	14.13
Effective grain size, D_{10} (mm)	0.20
D_{50} (mm)	0.30
D_{60} (mm)	0.32
Container 1	
Unit weight (kN/m^3)*	15.46
Density index (%)*	56
Friction angle, ϕ (°)†	31
Container 2	
Unit weight (kN/m^3)*	16.30
Density index (%)*	85
Friction angle, ϕ (°)†	41

*Estimated from four calibrated boxes placed on the bottom of each container.
†Measured from direct shear tests.

where Q_s is the shaft resistance; and Q_h is the uplift helix bearing capacity, which is expressed as

$$[4] \qquad Q_h = \sum_{i=1}^{N} Q_{hi}$$

where Q_{hi} is the uplift bearing capacity of the helix i.

There are two fundamental physical relationships in this proposed method. The first is between Q_s and T_s, and the second is between Q_h and T_h.

Relationship between Q_s and T_s

In the present model, the shaft resistance of helical piles under axial loading is represented by the shaft resistance derived from the torsional loading during pile installation. The relationship between Q_s and T_s, measured at the end of pile installation, can be given by the following equation:

$$[5] \qquad Q_s = \frac{2T_s}{d}$$

where d is the shaft external diameter.

According to Stoll (1972), who devised a simple field torque shear load test, the side friction measured by the torque tests should be on the conservative side when applied to axially loaded piles. Stoll compared the results of torque side shear capacity with the number of pile hammer blows and showed a reasonable relationship. As stated by Kelley and Lutenegger (2004), Q_s is the side friction along the entire side of the pile and is determined by multiplying the total pile surface area by unit skin friction (frictional resistance per unit area). Kelley and Lutenegger found similar results of skin friction data from standard penetration tests with torque measurement (SPT-T) and cone penetration test (CPT) sleeve measurements and backcalculated from pile loading tests. In their study, the skin friction (f_s) obtained from the rotation of the SPT split-barrel sampler is expressed as

$$[6] \qquad f_s = \frac{2T}{\pi d^2 L}$$

where T is the measured torque, d is the external diameter of the split-barrel sampler, and L is the length of penetration.

Zhang and Kong (2006) conducted centrifuge model tests to investigate the torsional behaviour of an instrumented model pile jacked into loose and dense sand. The average torsional shear resistance in the dense sand was slightly greater than the average axial shear resistance, and the average torsional shear resistance in the loose sand was slightly less than the average axial shear resistance. Zhang and Kong concluded that these differences occur because the horizontal stress is greater than the vertical stress in dense soil and less than the vertical stress in loose soil.

Based on the previous studies and considering that the differences between torsional and axial shear resistance measured by Zhang and Kong (2006) are irrelevant, it was assumed in the present approach that Q_s could be estimated by the required torque to rotate the shaft, as shown in eq. [5]. In this assumption, it was understood that the soil disturbance caused by the helix movement in a sand layer during installation equally affects the torsional and axial shear resistances on the shaft surface. The values of T_s can be calculated from eq. [5] after estimating Q_s by different methods presented in the geotechnical literature.

Relationship between Q_h and T_h

Ghaly et al. (1991) developed a theoretical model for screw anchors with one helical plate in dry sand from which the required installation torque can be determined in terms of the ultimate uplift resistance. They assumed that the applied torque is resisted by a system of forces acting on the upper surface of the screw element, which is the surface in contact with the sand due to screw rotation without downward advancement. Based on tests results, Weech (2002) concluded that the soil resistance to the downward penetration of the shaft of a helical pile into a sensitive fine-grained soil produces an upward thrust on the pile that must be compensated by downward resistance mobilized along the upper surface of the helix plates (since no external downward force is applied to the pile during installation). Both Ghaly et al. and Weech suppose that forces are mobilized on the upper surface of the helical plate during the helical pile installation. The model proposed in this study considers that the sum of these forces corresponds to Q_h shown in Figs. 1*b* and 2.

Figure 2 shows the resisting forces acting on the helix surfaces at a given installation depth. In this case, the pile is fixed at this level and prevented from downward advancement into the sand during the application of the torque. In Fig. 2, the force F_{at} is the frictional force acting on the screw blade, and the torque T_h is the resisting moment acting on the helices (also illustrated in Fig. 1*a*).

The physical relationship between Q_h and T_h presented in this paper is based on a mechanism frequently used in machine design, to the design of power screws, adapted for helical piles. In this adjustment shown in Fig. 3, the helical plate is equivalent to the screw helix, the surrounding sand to the nut, the residual friction angle between the helix material and surrounding sand δ_r to the friction angle between the screw helix material and the nut β, the load to be moved W to Q_h, and the resistant torque to the screw rotation against the load T to T_h.

The power screw design procedure was described in Faires (1943), who reported that, to obtain the torsional

Fig. 5. Model piles at the final embedded depth.

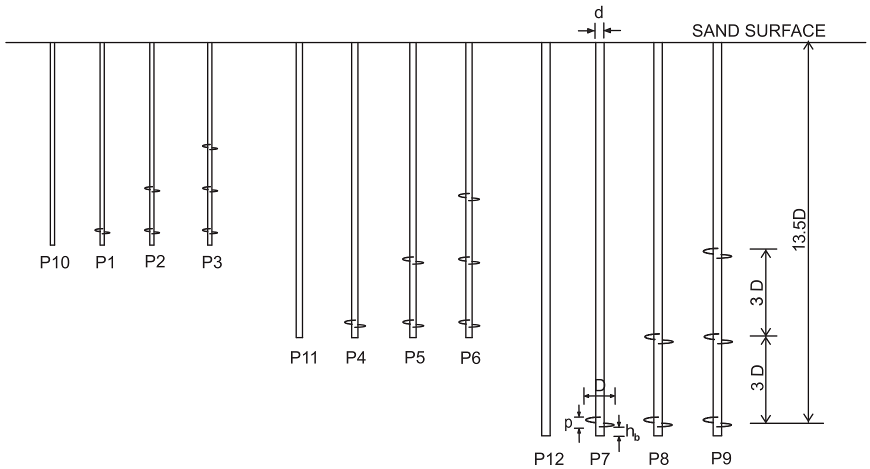

stress induced by turning the screw against a load, an expression must be derived for the twisting moment necessary to move the load. In this description, the surface of the screw thread may be thought of as an inclined plane wrapped around a cylinder. Figure 4*a* shows one thread unwrapped from the screw to get a simplest arrangement for a force analysis. In Fig. 4, the load is represented by a block (weighing *W*) resting on an inclined plane, and the height that the load moves in one turn is the pitch (for a single-thread screw). The forces acting on the block are *W* (Fig. 3), *Q* (which carries the weight up the plane), the frictional resistance (F_t), and the normal reaction *N*. The frictional resistance F_t and the normal reaction *N* combined give the total plane reaction (*R*).

Considering the forces acting on the block shown in Fig. 4*a*, the following equation can be written:

$$[7] \qquad W = \frac{Q}{\tan(\lambda + \beta)}$$

where *W* is the load to be moved, λ is the helix angle with the horizontal at D_m (Fig. 4*a*), *β* is the friction angle between the screw helix material and the nut, and *Q* is the force needed to move the load.

The torque required to rotate the screw against the load (*T*) is

$$[8] \qquad T = Q\frac{D_m}{2}$$

where D_m is the mean diameter of the screw, which can be given by the following equation:

$$[9] \qquad D_m = \frac{D + D_r}{2}$$

where *D* is the screw helix external diameter, and D_r is the screw helix internal diameter.

Substituting eq. [8] into eq. [7], the relationship between *W* and *T* can be expressed by the following equation:

$$[10] \qquad W = \frac{2T}{D_m \tan(\lambda + \beta)}$$

The weight *W* (Fig. 4*a*) is analogous to Q_h of the theoretical model presented in this work (Fig. 3). Figure 4*b* shows the adjustment of forces acting on the screw thread surface induced by turning the screw against a load (Fig. 4*a*) adapted for helical pile installation in sand.

Figure 4*b* shows that the resisting moment acting on the helix during pile installation is

$$[11] \qquad T_h = Q\frac{d_c}{2}$$

where d_c is the diameter of a circle corresponding to the helix surface area where the resisting forces are concentrated during pile installation.

The diameter of a circle corresponding to the helix surface area d_c and helix angle *θ* can be given by the following expressions:

$$[12] \qquad d_c = \frac{2}{3}\left(\frac{D^3 - d^3}{D^2 - d^2}\right)$$

$$[13] \qquad \theta = \tan^{-1}\left(\frac{p}{\pi d_c}\right)$$

where *d* is the shaft external diameter, and *p* is the helix pitch.

Equation [12] was published by Higdon and Stiles (1968) to calculate the ratio of a circle corresponding to the surface area of a disk clutch, subjected to a moment of frictional force, when the acting pressure is assumed to be uniformly distributed over the contact area. This expression was also used by Ghaly et al. (1991).

Equation [10], which is usually applied to the design of power screws, adapted for helical piles with one helical plate (Fig. 4*b*) in sand can be written as

$$[14] \qquad Q_h = \frac{2T_h}{d_c \tan(\theta + \delta_r)}$$

where *θ* is the helix angle with the horizontal at d_c, and δ_r is the residual interface friction angle between the helix material and surrounding sand.

Table 2. Dimensions of model and prototype piles.

Model pile	No. of helical plates	Diameter of pile shaft (mm)		Diameter of helical plate (mm)		Pitch of helical plate (mm)		Distance between pile toe and bottom helical plate (mm)		Prototype pile embedded depth (m)
		Model	Prototype	Model	Prototype	Model	Prototype	Model	Prototype	
P1	1	3.0	64.3	10	214	3.0	64.3	10	214	3.1
P2	2	3.0	64.3	10	214	3.0	64.3	10	214	3.1
P3	3	3.0	64.3	10	214	3.0	64.3	10	214	3.1
P4	1	4.5	97.7	15	326	3.2	69.5	10	217	4.6
P5	2	4.5	97.7	15	326	3.2	69.5	10	217	4.6
P6	3	4.5	97.7	15	326	3.2	69.5	10	217	4.6
P7	1	6.0	132.0	20	440	3.5	77.0	10	220	6.2
P8	2	6.0	132.0	20	440	3.5	77.0	10	220	6.2
P9	3	6.0	132.0	20	440	3.5	77.0	10	220	6.2
P10	—	3.0	64.3	—	—	—	—	—	—	3.1
P11	—	4.5	97.7	—	—	—	—	—	—	4.6
P12	—	6.0	132.0	—	—	—	—	—	—	6.2

Note: In this investigation, the model piles were installed at different depths, and therefore the following *g* levels were adopted to extrapolate the model pile dimensions to equivalent prototype values: 21.44*g* for piles P1, P2, P3, and P10; 21.71*g* for P4, P5, P6, and P11; 22.00*g* for P7, P8, P9, and P12.

As shown in Fig. 4, the residual friction angle between the helix material and sand δ_r is comparable to the friction angle between the screw material and the nut β. In view of the fact that the measured torque during pile installation comes from friction forces acting on the helix surface at relatively large displacements, Tsuha (2007) adopted the residual friction angle to be used in eq. [14].

By substituting eqs. [2] and [4] into eq. [14] to verify multi-helix pile capacity, it is noted that eq. [14] is identical for helical piles with one or more helical plates if the helical plates have equal dimensions (d_c and θ) and surrounding sand δ_r.

Relationship between Q_u and T

The relationship between Q_u and the components of the installation torque (T_s and T_h) was developed by substituting eqs. [5] and [14] into eq. [3]. As a result, this correlation proposed by Tsuha (2007) can be expressed by the following equation:

$$[15] \qquad Q_u = \frac{2T_s}{d} + \frac{2T_h}{d_c \tan(\theta + \delta_r)}$$

The first component of eq. [15] is Q_s represented by eq. [5], and the second component is Q_h represented by eq. [14].

As previously mentioned, during the inspection on site, the uplift capacity of helical piles must be controlled by the torque resistance measured during installation. Therefore, substituting eqs. [5] and [14] into eq. [1], the relationship between the torque value measured during the end of the pile installation T and the components of the uplift capacity Q_s and Q_h can be given by the following expression:

$$[16] \qquad T = \frac{Q_s d}{2} + \frac{Q_h d_c \tan(\theta + \delta_r)}{2}$$

The first component of eq. [16] is T_s represented by eq. [5], and the second component is T_h represented by eq. [14]. Equation [16] is applicable to piles with helical plates spaced a distance larger than three times the helix diameter to assure that the failure occurs above each individual helix.

Similar to eq. [14], eq. [16] is appropriate to control the uplift capacity of deep helical piles in sand, with one or more helical plates, when the helical plates have the same dimensions (d_c and θ) and surrounding sand δ_r. For helical piles with different helix diameters and surrounding sand, substituting eqs. [2] and [14] into eq. [16] gives

$$[17] \qquad T = \frac{Q_s d}{2} + \frac{\sum_{i=1}^{N} Q_{hi} d_{ci} \tan(\theta_i + \delta_{ri})}{2}$$

where d_{ci} is the diameter of a circle corresponding to the surface area of helix i, θ_i is the helix angle with the horizontal at d_{ci}, and δ_{ri} is the residual interface friction angle between helix material and surrounding sand at the depth of the helix i (when the pile penetrates sand layers of differing characteristics).

The use of eq. [16] or [17] is a simplified method to determine the final installation torque to control on site the uplift capacity of deep helical piles in sand.

To estimate T during the design phase using eq. [16] or [17], Q_s and Q_h can be calculated individually using methods described in the literature, and the residual interface friction angle between the helix material and the surrounding sand can be estimated using data of interface properties.

Centrifuge tests

Most of the previous studies on helical screw piles were conducted using scaled models tested at 1*g*. Levesque et al. (2003) was the first study on helical piles using centrifuge modeling reported in the literature. These centrifuge tests were carried out to investigate the cylindrical shear method for estimating uplift capacity of helical anchors in sand.

In the present study, a centrifuge modeling programme was performed at the Laboratoire Central des Ponts et

Table 3. Uplift capacities and final installation torques related to the contribution of helical plates in prototype values.

Model pile	No. of helical plates	Uplift helix bearing capacity (Q_h) in kN	Resisting moment acting on the helices (T_h) in kN·m
Container 1 (I_D = 56%)			
P1	1	14	0.3
P2	2	19	0.4
P3	3	43	1.0
P4	1	46	1.6
P5	2	83	3.2
P6	3	112	3.3
P7	1	69	4.1
P8	2	108	4.9
P9	3	150	5.3
Container 2 (I_D = 85%)			
P1	1	60	1.9
P2	2	88	2.8
P3	3	116	4.1
P4	1	177	7.7
P5	2	234	12.5
P6	3	275	10.7
P7	1	413	22.4
P8	2	475	35.1
P9	3	475	35.1

Table 4. Residual interface friction angles between helical plate material and sand samples.

	Residual interface friction angle, δ_r (°)	
	Sand (I_D = 56%)	Sand (I_D = 85%)
Steel plate	10.4	14.0
Welded plate	10.8	16.2
Average	10.6	15.1

Chaussées (LCPC) in France to validate eq. [14]. This equation, related to the contribution of helical plates to the uplift capacity, corresponds to the major component of the proposed relationship between uplift capacity and installation torque presented by eq. [15].

In this work, the first component of eq. [15], related to the shaft resistance of helical screw piles, was not verified by centrifuge tests because of the risk of scale effects on the results. Foray et al. (1998) reported that the diameter of a model pile should not be less than $200D_{50}$ (where D_{50} is the average grain size) to avoid any scale effects on shaft friction; in the present investigation, the ratio of shaft external diameter d to the average grain size D_{50} of the sand used varies from 10 to 20.

The relationship shown by eq. [14] contains five variables, namely d_c, θ, δ_r, Q_h, and T_h. In this investigation, d_c and θ values were determined by eqs. [12] and [13], respectively. The values of Q_h and T_h were obtained by centrifuge tests, and the values of δ_r by direct shear interface tests.

The tests were carried out at the LCPC centrifuge, which has a radius of 5.5 m, acceleration level of 200*g*, and payload of 2000 kg. Details of the LCPC centrifuge are given by Garnier et al. (1999).

Reconstituted samples of dry Fontainebleau sand were prepared by air pluviation technique using an automatic hopper. Tests were performed in two containers with dimensions equivalent to 1200 mm × 800 mm in plan area and a height of 340 mm. The containers were filled with sand samples of different densities (density index I_D = 56% and 85%). The physical properties of the sand samples are shown in Table 1.

Two different sets of reduced-scale model piles were fabricated for this study to isolate the parameters Q_h and T_h. In the first set (P1–P9 in Fig. 5), nine different piles were made with 0.75 mm thick steel helical plates welded to rounded steel bars. In the second set (P10–P12 in Fig. 5), three piles were made of rounded steel bars with different diameters. The model piles were 355 mm in length and had diameters of 3.0, 4.5, and 6.0 mm. The dimensions of the model piles and the corresponding prototypes are given in Table 2.

A total of 24 tests were carried out for this investigation. Twelve tests were performed in container 1 and reproduced in container 2.

A servocontrolled test system was used to install and pull out the model piles in the sand sample in-flight at 22*g*.

After the test apparatus was positioned, the model piles were installed in the soil in a smooth and continuous manner at a rotation rate of 5.3 rpm. The bottom helical plates of the first set of piles (P1–P9) were installed at a depth of 13.5 times the helix diameter. The embedded depth of the second set of piles (P10–P12) was determined according to the corresponding shaft diameter of the first set. After the pile was installed at the desired depth, a waiting sequence of at least 1 min was observed, and subsequently the pile was pulled vertically at a rate of 1 mm/s. As the model presented in this work is suggested to estimate the uplift capacity of helical piles, which generally corresponds to the maximum design load for a transient condition of short duration and occurs rarely during the life of the structure, it was considered that the displacement rate used in these tests is reasonable.

All piles tested in this research are classified as "deep piles" according to the definitions proposed by Meyerhof and Adams (1968). Details of the experimental apparatus and the experimental procedure were described in the preceding paper (Tsuha et al. 2007).

The torque required during pile installation was measured by a torquemeter, and the penetration depth and axial load were monitored by displacement and force transducers, respectively. The measures of torque, displacement, and force were recorded by an automatic data acquisition system placed in the centrifuge swinging basket.

The results of the centrifuge tests are presented as prototype values in Table 3. The parameters Q_h and T_h of all tested piles shown in this table were calculated by the difference between the test results of piles with a helix (P1–P9) and piles without a helix (P10–P12), both with the same diameter and embedded depth in soil (see Fig. 5). The values of the resisting moment acting on the helices T_h were measured at the end of the model pile installation.

Direct shear interface tests

Measured values of residual interface friction angle be-

Table 5. Physical properties of tested sands.

	Sand 1	Sand 2	Sand 3
Maximum dry density (kN/m^3)	15.88	15.32	16.54
Minimum dry density (kN/m^3)	13.68	13.62	14.42
Effective grain size, D_{10} (mm)	0.06	0.12	0.20
D_{50} (mm)	0.13	0.29	0.52
D_{60} (mm)	0.16	0.33	0.61
Particle shape	Subangular	Angular	Subangular

Table 6. Interface friction angles between the helix material of a typical helical screw pile and different surrounding sands.

Density index, I_D (%)	Residual interface friction angle, δ_r (°)
Sand 1 (D_{50} = 0.13 mm)	
25	18.8
55	19.8
85	20.7
Sand 2 (D_{50} = 0.29 mm)	
25	19.0
55	21.9
85	22.9
Sand 3 (D_{50} = 0.52 mm)	
25	15.9
55	19.0
85	20.6
Mean value of δ_r (°)	19.8
Standard deviation (°)	2.0
Coefficient of variation (%)	10

Note: The mean (±SD) value of δ_r is 19.8 ± 2.0, with a coefficient of variation of 10%.

tween the helix material and the surrounding sand are fundamental to validate eq. [14], which correlates Q_h with T_h.

Potyondy (1961) identified that the major factors that determine skin friction between soil and construction material are the moisture content of soils, the surface roughness of the material, the composition of soils, and the intensity of the normal load. Uesugi and Kishida (1986) declared that the frictional coefficient depends on surface roughness and sand type.

Abderrahim and Tisot (1993) concluded that the shearing resistance at the cohesionless soil–structure interface appreciably increases with an increase in the surface roughness of the structure. They also found that the residual resistance at the sand – smooth ring interface is very low (measured with the ring shear apparatus).

According to the research of Reddy et al. (2000), the interface friction angle cannot be expressed as a constant percentage of the internal friction angle of the soil and is a function of interface properties.

Consequently, direct shear interface tests were performed to determine the residual interface friction angle between the helix material and the surrounding sand δ_r used in centrifuge tests and between full-scale pile helical plates and different sand samples. The first part of this investigation was conducted at the LCPC in France, and the second part at the University of São Paulo in Brazil.

Part I: interface between helical plate material and sand samples used in centrifuge tests

Direct shear interface tests were performed with the Casagrande box using the same sand samples employed in the centrifuge tests. Because of the welding process, the helix surfaces of the model piles are constituted of steel and weld material. Considering the heterogeneity of the helix surfaces, the direct shear tests were conducted on samples of steel plates with and without welds. The sand was placed in the upper half of the box at the plate contact. These plates were dragged horizontally at a constant velocity. All model piles fabricated for this investigation present the welded surface (maximum roughness R_{max} = 4.7 μm) equivalent to approximately 50% of the value of the helix surface (R_{max} = 8.7 μm). Based on this assumption, the residual interface friction angle considered to verify eq. [14] is the average value of the results obtained in the steel and welded plate interface tests (Table 4).

Table 4 shows that the values of δ_r from the welded surface tests are slightly greater than those from the tests with no welded surfaces although the roughness of the welded surface is less than that of the steel helix surface. The welded surface has a lower hardness than the steel surface and thus the sand may have penetrated into the weld material during the tests. This conclusion is based on observation of the tested surfaces. After finishing the experiments, the welded surface was completely scratched.

Part II: interface between helical plate material used in field tests and different sand samples

The objective of this test program was to obtain values of residual interface friction angles between the helix material of a typical helical screw pile and different surrounding sands δ_r to be used in eq. [16] or [17] for helical piles with comparable sand–steel interface characteristics.

The research on frictional resistance of the interface between sand and steel reported by Uesugi and Kishida (1986) showed that the coefficient of friction is influenced by the steel roughness, the average grain size (D_{50}), and the sand type. Based on the reported previous experience, a sample of steel helical plate used in a typical helical screw pile (American Society for Testing and Materials (ASTM) standard A36 surface roughness R_{max} = 22.3 μm) was tested with three types of sand with different D_{50} values. The test equipment and procedure were the same as those used for the direct shear interface tests performed at the LCPC. Table 5 shows the physical properties of the tested sands.

The results of measured residual interface friction angles

Table 7. Comparison between measured and predicted uplift helix bearing capacity, Q_h.

Model pile	$Q_h$measured	Q_h predicted	$Q_{h\ measured}/Q_{h\ predicted}$
Container 1 (I_D = 56%)			
P1	14	12	1.17
P2	19	16	1.19
P3	43	40	1.08
P4	46	48	0.96
P5	83	96	0.86
P6	112	99	1.13
P7	69	97	0.71
P8	108	116	0.93
P9	150	125	1.20
Container 2 (I_D = 85%)			
P1	60	59	1.02
P2	88	87	1.01
P3	116	128	0.91
P4	177	178	0.99
P5	234	288	0.81
P6	275	247	1.11
P7	413	401	1.03
P8	475	628	0.76
P9	475	628	0.76

Fig. 6. Comparison between measured and predicted uplift helix bearing capacities (Tsuha et al. 2007).

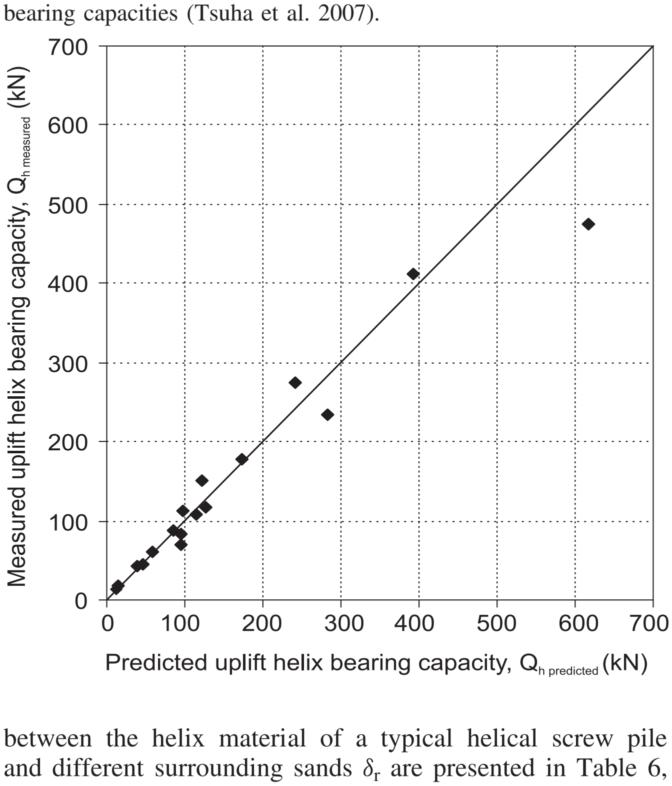

between the helix material of a typical helical screw pile and different surrounding sands δ_r are presented in Table 6, which shows that for this tested steel roughness the average grain size D_{50} did not influence the results of interface friction angles. This agrees with the conclusion drawn by Yoshimi and Kishida (1981), who stated that the frictional resistance between sand and a metal surface was primarily governed by the roughness of the metal surface.

The mean value of δ_r found in this test program is 19.8°, with a coefficient of variation of 10%. This value of δ_r is recommended for use in eq. [16] or [17] to control on site the uplift capacity of deep helical piles fabricated with ASTM A36 steel helical plates (or those with similar roughness) installed in sandy soils. In addition, Table 6 shows that in sand samples with larger D_{50} the sand relative density has a greater influence on the residual interface friction angle values.

Comparison of theoretical and experimental results

The uplift helix bearing capacity values from the aforementioned tests were compared with those predicted by eq. [14], where Q_h and T_h were measured by centrifuge modeling tests (Table 3) and the residual interface friction angles between between helix material and the surrounding sand δ_r were obtained by direct shear interface tests (Table 4).

The comparison between predicted and measured results is presented in Table 7 and Fig. 6. From this evaluation, it is apparent that there is a good agreement between the theoretical and experimental results. The mean value of $Q_{h\ measured}/Q_{h\ predicted}$ is 0.98, with a coefficient of variation of 15.7%.

In the present study, the measured values of uplift capacity and installation torque from the literature were not compared with those from the proposed relationship using eq. [16] (or eq. [17]) because the properties of sand–steel interfaces necessary to estimate the residual interface friction angle between helix material and surrounding sand δ_r were not available.

As the installation torque value estimated by the present relationship is considerably dependent on the residual interface friction angle between the helix material and the surrounding sand, it is essential to have reliable informationon the material properties of the sand and helical plate. One other limitation of the model is that it was not verified experimentally for the case of helical piles in saturated sand. On the other hand, Ghaly (1995) conducted installation and pull-out tests on model screw anchors with one helical plate in dry and saturated sand and found that the installation torque and uplift capacity are lower in saturated sand. However, Ghaly obtained similar values of the ratio between uplift capacity and installation torque from tests on deep piles (ratio of helix depth to helix diameter > 10) installed in dry and saturated sand at the same depth.

Torque correlation factor in sandy soils

The torque correlation factor (K_T) indicates the magnitude of the relationship between uplift capacity and installation torque of helical screw piles.

Hoyt and Clemence (1989) noted that this empirical factor has been used successfully in the construction of thousands of anchors over the past 20 years and described the uplift capacity calculated from installation torque as

$$Q_u = K_T T \quad [18]$$

where K_T is equal to 33 m^{-1} for all square-shaft anchors and round-shaft anchors less than 89 mm in diameter, 23 m^{-1} for 89 mm diameter round-shaft anchors, and 9.8 m^{-1} for anchors with 219 mm diameter extension shafts; and T is the

Table 8. Measured torque correlation factor, K_T (Tsuha 2007).

Model pile	Prototype helical plate diameter, D_P (mm)	No. of helical plates	Uplift helix bearing capacity (Q_h) in kN	Resisting moment acting on the helices (T_h) in kN·m	K_T (= Q_h/T_h) in m^{-1}
Container 1 (I_D = 56%)					
P1	214	1	14	0.3	47
P2	214	2	19	0.4	48
P3	214	3	43	1.0	43
P4	326	1	46	1.6	29
P5	326	2	83	3.2	26
P6	326	3	112	3.3	34
P7	440	1	69	4.1	17
P8	440	2	108	4.9	22
P9	440	3	150	5.3	28
Container 2 (I_D = 85%)					
P1	214	1	60	1.9	32
P2	214	2	88	2.8	31
P3	214	3	116	4.1	28
P4	326	1	177	7.7	23
P5	326	2	234	12.5	19
P6	326	3	275	10.7	26
P7	440	1	413	22.4	18
P8	440	2	475	35.1	14
P9	440	3	475	35.1	14

average installation torque (the installation torque should be averaged for the final distance of penetration equal to three times the diameter of the largest helix).

Torque factor measured in centrifuge tests

As already reported in this paper, the results of the shaft resistance acting during pile installation and pull-out tests, measured by the centrifuge investigation performed in this study, were affected by scale effects. However, it was observed from these results that the fractions of uplift capacity and installation torque associated with the resistance on the pile shaft, considering the scale effects according to Garnier and König (1998), are not significant in this investigation compared with the helix contribution to the uplift capacity and the resisting moments acting during pile installation. Based on this assumption, the values of K_T were determined in this investigation by dividing Q_h by T_h measured at the end of pile installation. The results are presented in Table 8.

The A.B. Chance Co. (1994) reported that K_T may range from 10 to 66 m^{-1}, depending on soil conditions and helical pile design; and the values of K_T found in the present study range from approximately 14 to 48 m^{-1} (Table 8).

Table 8 shows that the K_T values decrease with an increase in sand relative density and helical plate diameter. Taking into account that δ_r increases with an increase in the sand relative density (see Tables 4, 6), K_T thus decreases with an increase in δ_r. Also, as d_c (see eq. [12]) increases with an increase in the helical plate diameter D, then K_T decreases with an increase in d_c.

These previous observations are confirmed by eq. [19], which is obtained by substituting eq. [14] into eq. [18] (as there is no shaft resistance in this case, it was considered that $Q_u = Q_h$ and $T = T_h$). As a result, K_T is

$$[19] \qquad K_T = \frac{2}{d_c \tan(\theta + \delta_r)}$$

In addition, Table 8 shows that K_T is not correlated with the number of helical blades, which agrees with the experience of Hargrave and Thorsten (1992) with helical piers in expansive soils. This fact is also confirmed by eq. [19], which shows that K_T does not depend on the number of helices.

As with eq. [14], eq. [19] is suggested for deep helical piles in sand with identical helix dimensions (d_c and θ) and surrounding sand δ_r when the fractions of the uplift capacity and installation torque associated with the resistance on the pile shaft are not significant. In cases where the shaft resistance is significant, K_T must be obtained by substituting eq. [16] into eq. [18]. As a result, K_T can be expressed by the following equation:

$$[20] \qquad K_T = \frac{2}{\left(\frac{Q_s}{Q_u}\right) d + \left(\frac{Q_h}{Q_u}\right) d_c \tan(\theta + \delta_r)}$$

The torque factor K_T for helical piles with different helix diameters and surrounding sand can be found by substituting eq. [17] into eq. [18], as illustrated by the following expression:

$$[21] \qquad K_T = \frac{2}{\left(\frac{Q_s}{Q_u}\right) d + \sum_{i=1}^{N} \left(\frac{Q_{hi}}{Q_u}\right) d_{ci} \tan(\theta_i + \delta_{ri})}$$

Equations [19], [20], and [21] show the physical mean for deep helical piles embedded in sand of the empirical relationship K_T usually used as an instrument to control on site the uplift capacity.

Table 9. Values of torque correlation factor (K_T) found in the literature.

Reference	Depth of top helical plate	No. of helical plates	Pile dimensions (mm)	Soil	Torque correlation factor, K_T (m^{-1})
Centrifuge model tests					
Tsuha (2007)	7.5D–13.5D	1–3	D = 214–440*; d = 64.3–132	Dry sand; ϕ = 31°	17–48
Tsuha (2007)	7.5D–13.5D	1–3	D = 214–440*; d = 64.3–132	Dry sand; ϕ = 41°	14–32
Full-scale field tests					
Adams and Klym (1972)	12.6D	2	D = 203, 254; d = 89	Dry silty sand; ϕ = 40°	16
Mitsch and Clemence (1985)	8D	3	D = 203, 253, 287; d = 38	Dry sand; ϕ = 35°–40°	49–81
Zhang (1999)	10.7D	2; 3	D = 356; d = 219	Dry sand; ϕ = 39°	7
Tsuha (2007)	44D	2	D = 254, 305; d = 95	Saturated clayed sand; ϕ = 32°	24
Livneh and El Naggar (2008)	17.3D; 26.3D	3	D = 200, 250, 300; d = 44.5	Saturated sand; ϕ = 38°	24.3; 32.7
Small-scale laboratory model tests					
Mitsch and Clemence (1985)	8D	1; 3	D = 96 and D = 68, 84, and 96; d = 44.5	Dry sand; ϕ = 35°	83–128
Mitsch and Clemence (1985)	8D	1; 3	D = 96 and D = 68, 84, and 96; d = 44.5	Dry sand; ϕ = 46°	47–60
Ghaly et al. (1991)	8D–16D	1†	D = 50; d = 18	Dry sand; ϕ = 30°	60–90
Ghaly et al. (1991)	8D–16D	1†	D = 50; d = 18	Dry sand; ϕ = 35°	80–110
Ghaly et al. (1991)	8D–16D	1†	D = 50; d = 18	Dry sand; ϕ = 40°	79–107
Ghaly and Hanna (1991)	8D–16D	1†	D = 50; d = 16	Dry sand; ϕ = 31°	253–304
Ghaly and Hanna (1991)	8D–16D	1†	D = 50; d = 16	Dry sand; ϕ = 36°	241–281
Ghaly and Hanna (1991)	8D–16D	1†	D = 50; d = 16	Dry sand; ϕ = 42°	167–226
Ghaly (1995)	8D–16D	1	D = 50; d = 18	Dry sand; ϕ = 40°	78–107
Ghaly (1995)	8D–16D	1	D = 50; d = 18	Saturated sand; ϕ = 40°	55–107

*Pile prototype dimensions; multi-helix piles fabricated with helices of the same diameter.
†Only the piles with a single medium-pitch screw were considered.

Fig. 7. Comparison of measured torque correlation factors, K_T.

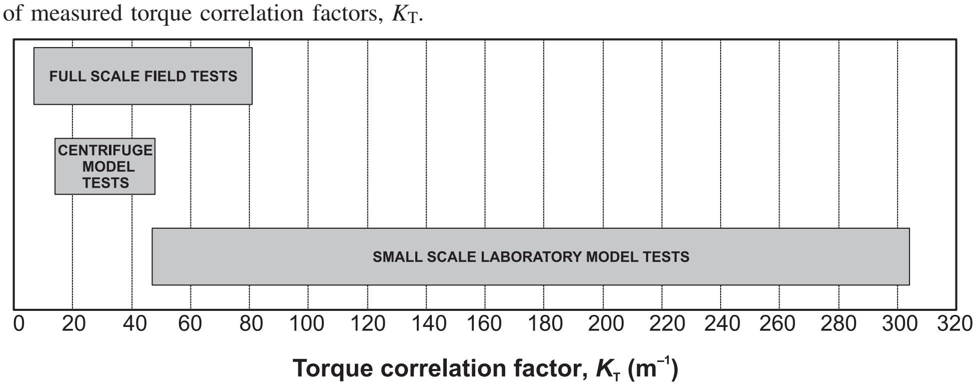

Comparison with K_T values in the literature

A set of K_T values are reported in the literature for single- and multi-helix deep helical piles installed in sand. Table 9 presents some of the values obtained from small-scale laboratory models and full-scale field tests.

Table 9 and Fig. 7 show that measured values of K_T ranged from 47 to 304 m^{-1} for small-scale laboratory tests and from 7 to 81 m^{-1} for centrifuge modeling and full-scale field tests. This shows that the pile dimension significantly influences K_T. This observation can be explained by eqs. [20] and [21], which show that K_T increases with a decrease in helical plate diameter (d_c) and shaft diameter (d).

As the helix–sand interface properties required to deduce the residual interface friction angle between the helix material and the surrounding sand δ_r were not presented in Table 9, the influence of δ_r on K_T was verified by comparing the sand friction angle ϕ available in these tests. From this comparison, it was demonstrated that the magnitude of K_T decreases with an increase in ϕ for the same tested pile (see Table 9 for the centrifuge tests of Tsuha (2007) and the laboratory tests of Mitsch and Clemence (1985) and Ghaly and Hanna (1991)). In contrast, the results of Ghaly et al. (1991) show that ϕ does not affect the values of K_T. The present authors suppose that this occurs because, for the tested pile, the friction angle between the helix material and the surrounding sand δ_r was not influenced by ϕ. A similar result was observed in the tested interface between helical plate material and different sand samples presented in this study (see Table 6). In these tests, the relative density (consequently ϕ) weakly affected the results of δ_r.

Considering the cases where K_T decreases with an increase in ϕ (Table 9), and for these tested interfaces, δ_r increases with an increase in ϕ, it can be confirmed that K_T decreases with an increase in δ_r, as demonstrated by the proposed model in eqs. [20] and [21].

In addition and as noted in Table 9, Ghaly et al. (1991) and Ghaly and Hanna (1991) performed tests with similar pile dimensions and sand friction angles, and the K_T values determined by Ghaly and Hanna are considerably greater that those determined by Ghaly et al. The present authors believe that this occurred because the tests were performed with different helix–sand interface characteristics.

Conclusions

Research was conducted to evaluate the physical relationship between the uplift capacity and installation torque of deep helical piles in sand. Based on the results of the present investigation, the following conclusions are drawn:

(1) A simplified theoretical expression was developed to correlate the uplift capacity with the torque required to install deep helical piles in sand.
(2) The component of the proposed relationship related to the contribution of the helical plates to the uplift capacity was verified by centrifuge physical modeling.
(3) A comparison of uplift helix bearing capacity from theoretical and experimental results showed good agreement between predicted and measured values.
(4) Results of residual interface friction angles between helix material of a typical helical screw pile and different surrounding sands were presented for use in the proposed relationship for piles with similar sand–steel interface characteristics.
(5) The measured values of the torque correlation factor (K_T) obtained in this study were compared with field and laboratory results reported in the literature. From this evaluation, it can be seen that the magnitude of K_T decreases with an increase in pile dimensions and also sand friction angle (when the residual friction angle δ_r is influenced by the sand friction angle ϕ).
(6) The values of K_T found in this investigation and in the literature review are explained by the relationship recommended in this paper.

Acknowledgements

This research was supported by the Laboratoire Central des Ponts et Chaussées, France, Vértice Engenharia, Brazil, and the Brazilian Agency CAPES (Ministry of Education). The authors thank the following colleagues for valuable assistance with centrifuge physical modeling: Jacques Garnier, Luc Thorel, and Gerard Rault.

References

A.B. Chance Co. 1994. Helical pier foundation systems. Technical Manual. Bulletin 01-9601, A.B. Chance Co., Centralia, Mo.

Abderrahim, A., and Tisot, J.P. 1993. Friction at the cohesionless soil–structure interface: effect of various parameters according to a classic study and a new approach. Geotechnical Testing Journal, **16**(1): 122–130. doi:10.1520/GTJ10275J.

Adams, J.I., and Klym, T.W. 1972. A study of anchors for transmission tower foundations. Canadian Geotechnical Journal, **9**(1): 89–104. doi:10.1139/t72-007.

Clemence, S.P., Crouch, L.K., and Stephenson, R.W. 1994. Prediction of uplift capacity for helical anchors in sand. *In* Proceedings of the 2nd Geotechnical Engineering Conference, Cairo, Egypt.

Faires, V.M. 1943. Design of machine elements. Revised edition. Macmillan Company, New York.

Foray, P., Balachowski, L., and Rault, G. 1998. Scale effects in shaft friction due the localization of deformations. *In* Proceedings of the International Conference Centrifuge 98, Tokyo, Japan, 23–25 September 1998. *Edited by* T. Kimura, O. Kusakabe, and J. Takemura. A.A. Balkema, Rotterdam, the Netherlands. Vol. 1, pp. 211–216.

Garnier, J., and König, D. 1998. Scale effects in piles and nails loading tests in sand. *In* Proceedings of the International Conference Centrifuge 98, Tokyo, Japan, 23–25 September 1998. *Edited by* T. Kimura, O. Kusakabe, and J. Takemura. A.A. Balkema, Rotterdam, the Netherlands. Vol. 1, pp. 205–210.

Garnier, J., Derkx, F., Cottineau, L.M., and Rault, G. 1999. Études géotechniques sur modéles réduits centrifugés — Evolution des matériels et techniques expérimentales. Bulletin des Laboratoires des Ponts et Chaussées, No 223, pp. 27–50.

Ghaly, A.M. 1995. Drivability and pullout resistance of helical units in saturated sands. Soils and Foundations, **35**(2): 61–66.

Ghaly, A., and Hanna, A. 1991. Experimental and theoretical studies on installation torque of screw anchors. Canadian Geotechnical Journal, **28**(3): 353–364. doi:10.1139/t91-046.

Ghaly, A., Hanna, A., and Hanna, M. 1991. Installation torque of screw anchors in sand. Soils and Foundations, **31**(2): 77–92.

Hargrave, R.L., and Thorsten, R.E. 1992. Helical piers in expansive soils of Dallas, Texas. *In* Proceedings of the 7th International Conference on Expansive Soils, Dallas, Tex., 3–5 August 1992. Texas Tech University Press, Lubbock, Tex. Vol. 1, pp. 125–130.

Higdon, A., and Stiles, W.B. 1968. Engineering mechanics. Vol. 1. 3rd Ed. Prentice-Hall, Englewood Cliffs, N.J.

Hoyt, R.M., and Clemence, S.P. 1989. Uplift capacity of helical anchors in soil. *In* Proceedings of the 12th International Conference on Soil Mechanics and Foundation Engineering, Rio de Janeiro, 13–18 August 1989. A.A. Balkema, Rotterdam, the Netherlands. Vol. 2, pp. 1019–1022.

Kelley, S.P., and Lutenegger, A.J. 2004. Unit skin friction from the Standard Penetration Test supplemented with the measurement of torque. Journal of Geotechnical and Geoenvironmental Engineering, ASCE, **130**(5): 540–543. doi:10.1061/(ASCE)1090-0241(2004)130:5(540).

Levesque, C.L., Wheaton, D.E., and Valsangkar, A.J. 2003. Centrifuge modeling of helical anchors in sand. *In* Proceedings of the 12th Panamerican Conference on Soil Mechanics and Foundation Engineering, Boston, Mass., 22–26 June 2003. *Edited by* P.J. Culligan, H.H. Einstein, and A.J. Whittle. Massachusetts Institute of Technology (MIT), Cambridge. Vol. 2, pp. 1859–1864.

Livneh, B., and El Naggar, M.H. 2008. Axial testing and numerical modeling of square shaft helical piles under compressive and tensile loading. Canadian Geotechnical Journal, **45**(8): 1142–1155. doi:10.1139/T08-044.

Meyerhof, G.G., and Adams, J.I. 1968. The ultimate uplift capacity of foundations. Canadian Geotechnical Journal, **5**(4): 225–244. doi:10.1139/t68-024.

Mitsch, M.P., and Clemence, S.P. 1985. The uplift capacity of helix anchors in sand. *In* Uplift Behavior of Anchor Foundations in Soil: Proceedings of a Session sponsored by the Geotechnical Engineering Division of the American Society of Civil Engineers in Conjunction with the ASCE Convention in Detroit, Mich., 24 October 1985. ASCE, New York. pp. 26–47.

Narasimha Rao, S., Prasad, M.D., Shetty, M.D., and Joshi, V.V. 1989. Uplift capacity of screw pile anchors. Geotechnical Engineering, **20**(2): 139–159.

Pack, J.S. 2003. Helical foundation and tiebacks: quality control, inspection and performance monitoring. *In* Proceedings of the 28th Annual Conference on Deep Foundations, Miami Beach, Fla. Deep Foundations Institute, Hawthorne, N.J. pp. 269–284.

Perko, H.A. 2000. Energy method for predicting the installation torque of helical foundations and anchors. *In* New technologiesl and design developments in deep foundations. *Edited by* N.D. Dennis, Jr., R. Casteli, and M.W. O'Neill. ASCE Press, Reston, Va. pp. 342–352.

Potyondy, J.G. 1961. Skin friction between various soil and construction materials. Géotechnique, **II**(4): 339–353.

Reddy, E.S., Chapman, D.N., and Sastry, V.V.R.N. 2000. Direct interface test for shaft capacity of piles in sand. Geotechnical Testing Journal, **23**(2): 199–205. doi:10.1520/GTJ11044J.

Stoll, U.W. 1972. Torque shear test of cylindrical friction piles. Civil Engineering, ASCE, **42**(4): 63–64.

Tsuha, C.H.C. 2007. Theoretical model to control on site the uplift capacity of helical screw piles embedded in sandy soil. Ph.D. thesis, Department of Geotechnics, São Carlos School of Engineering, University of São Paulo, São Carlos, Brazil. [In Portuguese.]

Tsuha, C.H.C., Aoki, N., Rault, G., Thorel, L., and Garnier, J. 2007. Physical modeling of helical pile anchors. International Journal of Physical Modelling in Geotechnics, **7**(4): 1–12.

Uesugi, M., and Kishida, H. 1986. Frictional resistance at yield between dry sand and mild steel. Soils and Foundations, **26**(4): 139–149.

Weech, C.N. 2002. Installation and load testing of helical piles in a sensitive fine-grained soil. M.A.Sc. thesis, Department of Civil Engineering, The University of British Columbia, Vancouver, B.C.

Yoshimi, Y., and Kishida, T. 1981. Friction between sand and metal surface. *In* Proceedings of the 10th International Conference on Soil Mechanics and Foundation Engineering, Stockholm, Sweden, 15–19 June 1981. A.A. Balkema, Rotterdam, the Netherlands. Vol. 1, pp. 831–834.

Zhang, D.J.Y. 1999. Predicting capacity of helical screw piles in Alberta soils. M.Sc.E. thesis, Department of Civil and Environmental Engineering, University of Alberta, Edmonton, Alta.

Zhang, L.M., and Kong, L.G. 2006. Centrifuge modeling of torsional response of piles in sand. Canadian Geotechnical Journal, **43**(5): 500–515. doi:10.1139/T06-020.